RELAXED INCREMENTAL FORMULATIONS FOR DAMAGE AT FINITE STRAINS INCLUDING STRAIN SOFTENING

M. KÖHLER*, T. NEUMEIER†, D. PETERSEIM‡, M. A. PETER‡, D. BALZANI*

Abstract. Relaxation is a promosing technique to overcome mesh-dependency in computational damage mechanics originating from the non-convexity of an underlying incremental variational formulation. This technique does not require an internal length scale parameter. However, in case of damage formulations, for many years the decrease of stresses with an increase of strains, referred to as strain-softening, could not be modeled in the relaxed regime. This contribution discusses several possibilities of relaxation that lead to suitable models for stress- and strain-softening.

1. Introduction

Materials undergoing dissipative processes can be mathematically formulated in terms of the incremental variational framework which has been introduced by a series of papers, see e.g., [1, 2, 3, 4, 5]. This powerful framework yields pseudo-elastic potentials which are thermodynamically consistent per incremental step. However, the resulting potentials exhibit non-convexity, which leads to ill-posedness of the finite element discretization. For detailed information, the interested reader is referred to [6, Sec. 9.2.3]. The technique of relaxation overcomes this issue by replacing the incremental stress potential (also called reduced or condensed energy) by a (semi)convex envelope.

Relaxation methods in continuum mechanics began to develop in the fields of plasticity and phase transition problems, see e.g., [7, 8, 9]. The first application in continuum damage mechanics was in the small strain regime by [10]. There, the phenomenological scalar-valued continuum damage mechanics approach that dates back to [11, 12] was relaxed for simplified one-dimensional cases even though the resulting response was multi-dimensional. In [13], the relaxation case was extended to the finite strain setting; however, the relaxation was still restricted to one-dimensional models for fibrous materials that were homogenized to obtain a multi-dimensional response. Both contributions relaxed the problem whenever the original incremental stress potential lost its convexity and afterwards kept the convex hull fixed. Since convexity implies a linear connection of two supporting points of the convex hull, none of the two approaches could model strain softening, since the stresses are the first derivative of the incremental stress potential and, thus, constant

* Chair of Continuum Mechanics, Ruhr University Bochum, Universitätsstr. 150, 44801 Bochum, Germany

† Institute of Mathematics, University of Augsburg, Universitätsstr. 12a, 86159 Augsburg, Germany

‡ Institute of Mathematics & Centre for Advanced Analytics and Predictive Sciences (CAAPS), University of Augsburg, Universitätsstr. 12a, 86159 Augsburg, Germany

E-mail address: {daniel.balzani, maximilian.koehler}@rub.de, timo.neumeier@uni-a.de, {malte.peter, daniel.peterseim}@uni-a.de.

Date: November 24, 2022.

We acknowledge the Deutsche Forschungsgemeinschaft (DFG) for funding within the Priority Program 2256 ("Variational Methods for Predicting Complex Phenomena in Engineering Structures and Materials"), project ID 441154176, reference IDs BA2823/17-1, PE1464/7-1, and PE2143/5-1. Further, the free and open source community of Julia is acknowledged.

within the convexified regime. Further, the construction of the convex envelope was a sophisticated problem since it is a two-dimensional multi-modal optimization problem in the finite strain setting. In order to obtain the global minimum, a multistart Newton strategy was employed in [13] that was later extended in [14] by an evolution strategy for the multistart points.

Recently, the contribution [15] approached the problem differently by emulating microstructures instead of detecting supporting points of the convex hull. This is possible due to the fact that the supporting points of the convex envelope are minimizers of the original problem that describe homogenized microstructures. There, the emulated microstructure was allowed to evolve which made it possible to describe strain softening. An outstanding feature of this contribution is that relaxation is realized in the multi-dimensional setting. However, the emulation of the microstructures requires assumptions and the obtained relaxed energy is a convex envelope which neglects compatibility. Due to the discrete convexification scheme of [16], the construction of a one-dimensional convex envelope is significantly accelerated. This can be exploited in the one- and multi-dimensional relaxation setting. Within this contribution, two approaches are shown that allow for the description of strain softening. Namely, the construction of rank-one convex envelopes in the multi-dimensional setting by methods from [17, 18] as well as the evolution of the convex envelope in the one-dimensional relaxation setting which is reported in detail in [19]. In contrast to existing methods, the obtained supporting points and thus the implied homogenized microstructures converge to the mechanically correct solution of the problem.

2. Relaxation

The incremental stress potential of the scalar-valued phenomenological approach of continuum damage mechanics was derived in detail in [13] and has the closed form

$$W(\boldsymbol{F}) = \psi(\boldsymbol{F}, D) - \psi(\boldsymbol{F}_k, D_k) + \beta D - \beta_k D_k - \tilde{D} + \tilde{D}_k. \tag{1}$$

Therein, ψ denotes the strain energy density

$$\psi(\boldsymbol{F}^T\boldsymbol{F}, D(\beta)) = (1 - D(\beta))\,\psi^0(\boldsymbol{F}^T\boldsymbol{F}), \tag{2}$$

where ψ^0 denotes the virtually undamaged strain energy density of the material. The internal variable

$$\beta := \max_{s \le t} \left[\psi^0(\boldsymbol{F}^T\boldsymbol{F})\right] \tag{3}$$

maps to a damage variable D by the monotonically increasing damage function $D(\beta)$,

$$D(\beta) = D_\infty \left[1 - \exp\left(\frac{-\beta}{D_0}\right)\right]. \tag{4}$$

Within the incremental stress potential, $\tilde{D}$ describes the antiderivative of the damage function and the subscript k denotes the value of the previous time increment. Whenever W looses convexity it is replaced by its (semi)convex envelope. Since in one-dimension all semiconvex notions (i.e. polyconvexity, rank-one convexity, and quasiconvexity) coincide with convexity, the problem reduces in the one-dimensional setting to

$$W \leftarrow W^{\mathrm{c}}(F) = \inf_{F^+, F^-} [\bar{W}(F)] \tag{5}$$

with

$$\bar{W}(F) = \xi W(F^+) + (1 - \xi) W(F^-) \quad \text{and} \quad \xi = \frac{F - F^-}{F^+ - F^-}. \tag{6}$$

This problem can be efficiently solved by the discrete convexification scheme reported in [16] with linear complexity.

The multi-dimensional setting is more sophisticated, since the chosen (semi)convex notion drastically influences the complexity of the construction of the associated hull. While performant convex hull construction algorithms exists, convexity is in general a too strict notion that violates continuum mechanical requirements, see e.g. [20, Section A.5]. Quasiconvex and polyconvex hulls are in general hard to obtain, because in the prior case only an integral condition exists and for the latter case, sophisticated constraints of the semiconvex hull supporting points are present. In addition, rank-one convex hulls are the closest to the original function and, thus, encode the most features of the original function which is of great importance later. Therefore, we resort the relaxation in the multi-dimensional case to rank-one convexity. Rank-one convexity can be expressed as follows

$$W(\xi\,\boldsymbol{F}^+ + (1-\xi)\,\boldsymbol{F}^-) \leq \xi\,W(\boldsymbol{F}^+) + (1-\xi)\,W(\boldsymbol{F}^-) \tag{7}$$

for all $\xi \in [0,1]$ and $\boldsymbol{F}^+, \boldsymbol{F}^- \in \mathbb{R}^{d\times d}$ with $\operatorname{rank}(\boldsymbol{F}^+ - \boldsymbol{F}^-) = 1$. Using the recursive formulation based on the idea of successive lamination, this can be recast into an optimization problem for the rank-one convex hull by

$$W^{\mathrm{rc}}_{k+1}(\boldsymbol{F}) = \inf\left\{\xi\,W^{\mathrm{rc}}_k(\boldsymbol{F}^+) + (1-\xi)W^{\mathrm{rc}}_k(\boldsymbol{F}^-)\;\middle|\;\begin{smallmatrix}\boldsymbol{F}=\xi\boldsymbol{F}^+ + (1-\xi)\boldsymbol{F}^-,\\ \xi\in[0,1],\,\operatorname{rank}(\boldsymbol{F}^+-\boldsymbol{F}^-)=1\end{smallmatrix}\right\}. \tag{8}$$

The idea was presented in [21, Section 5C] and starts for $k=0$ with $W^{\mathrm{rc}}_0(\boldsymbol{F}) = W(\boldsymbol{F})$ and converges for $k\to\infty$ against the rank-one convex hull. The index k refers to the k-th lamination iteration and represents at the same time the highest possible laminate order.

3. Numerical Rank-One Convexification

Parametrizing the deformation gradient for the multi-dimensional relaxation case yields again a non-convex multi-dimensional and multi-modal optimization problem with the addition of challenging constraints. Moreover, the optimization problem needs to be solved multiple times depending exponentially on the chosen lamination depth. This issue can be circumvented by methods which utilize the fact that rank-one convexity corresponds to convexity along rank-one lines. Across rank-one lines, performant one-dimensional relaxation methods can be used as presented in [16]. This idea originates from [17] and was extended in [18]. Both contributions first discretize the deformation gradient space

$$\mathcal{N}_{\delta,r} = \delta\,\mathbb{Z}^{d\times d} \cap \left\{\boldsymbol{F}\in\mathbb{R}^{d\times d}\mid\ |\boldsymbol{F}|_\infty \leq r\right\}, \tag{9}$$

where d, δ and r denote the physical dimensions, convexification grid size and radius, respectively. The extension of [18] to [17] lies in the discretization of the rank-one directions

$$\mathcal{R}^1_{\delta,r} = \{\boldsymbol{a}\otimes\boldsymbol{b}\mid \boldsymbol{a},\boldsymbol{b}\in\delta\,\mathbb{Z}^d, |\boldsymbol{a}|\leq 2dr, 1-d\delta\leq|\boldsymbol{b}|\leq 1+d\delta\}, \tag{10}$$

which are defined depending on the chosen convexification grid. Namely, the definition covers all present rank-one directions within the grid. Further, [18] introduced a linear interpolation operator, such that an independent convolution for each $\boldsymbol{F}\in\mathcal{N}_{\delta,r}$ with a linear optimization problem of the form

$$W^\delta_{k+1}(\boldsymbol{F}) = \inf\left\{\xi W^\delta_k(\boldsymbol{F}+\delta l_1\boldsymbol{A}) + (1-\xi)W^\delta_k(\boldsymbol{F}+\delta l_2\boldsymbol{A})\;\middle|\;\begin{smallmatrix}\boldsymbol{A}\in\mathcal{R}^1_{\delta,r},\,\xi\in[0,1],\,l_1,l_2\in\mathbb{Z},\\ \xi l_1+(1-\xi)l_2=0\end{smallmatrix}\right\}, \tag{11}$$

can be realized. Here, $W^\delta_0 = I_\delta(W(\boldsymbol{F}))$ denotes the linear interpolation with the interpolation points $\mathcal{N}_{\delta,r}$. An application of the algorithm for $d\times d$ matrices and $d=2$ can be seen in Figure 1. In this example a St. Venant–Kirchhoff effective energy ψ^0 has been used. Within this figure, the top part shows the starting non-convex incremental stress potential $W(\boldsymbol{F})$ and the resulting approximation of the rank-one convex hull $W^{\mathrm{rc}}_{20}(\boldsymbol{F})$.

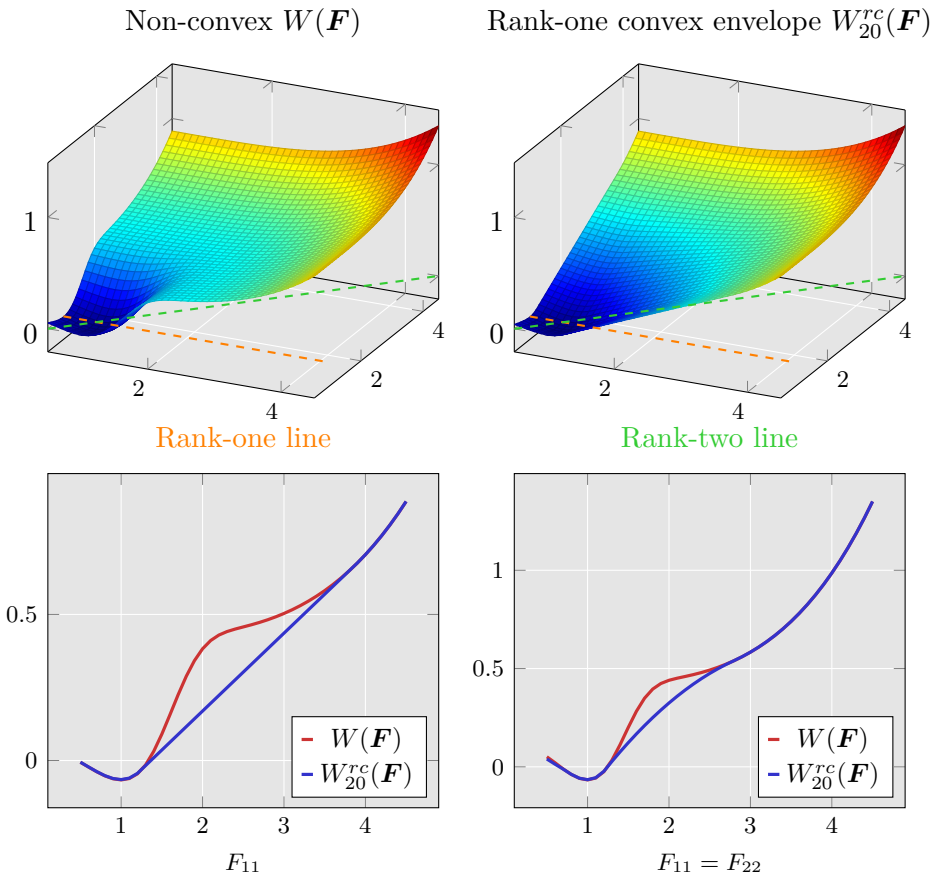

FIGURE 1. Incremental stress potential $W(\boldsymbol{F})$ at the top left-hand side with the corresponding high order lamination $k = 20$ approximated rank-one convex hull $W^{\text{rc}}_{20}(\boldsymbol{F})$ at the top right-hand side within the $F_{11} - F_{22}$ plane. Here, a St. Venant–Kirchhoff effective ψ^0 was used which is not polyconvex. At the bottom left-hand side, a rank-one line evaluation for the original non-convex $W(\boldsymbol{F})$ and approximated rank-one convex hull $W^{\text{rc}}_{20}(\boldsymbol{F})$ can be seen which is convex for the rank-one convex hull. The bottom right-hand side shows an evaluation along a rank-two line for both functions, where also non-convexity for the rank-one convex envelope can be observed. However, rank-one convexity turns out to reduce the non-convexity along a rank-two line.

After 20 lamination iterations, the algorithm was stopped. For the convexification grid, 8649 points were used with three points along each off-diagonal axis and 31 points for each diagonal axis. At the bottom part of the figure, two parameterized deformation paths and their associated values of the incremental stress potential with the rank-one convex envelope are shown. The parameterized deformation paths have different ranks and are of the form

$$\boldsymbol{F}^{r1} = \begin{bmatrix} \lambda_1 & 0 \\ 0 & 1 \end{bmatrix} \qquad \boldsymbol{F}^{r2} = \begin{bmatrix} \lambda_2 & 0 \\ 0 & \lambda_2 \end{bmatrix} \qquad \text{with} \qquad \lambda_1, \lambda_2 \in (0, 4.3]. \tag{12}$$

The prior is visualized as an orange dashed line, while the latter is a green dashed line in the surface plots of Figure 1. As observable in the $\boldsymbol{F}^{r1}$ parameterized path, the obtained approximation of the rank-one convex envelope is convex, whereas the original incremental

stress potential is not. Notably, the $\boldsymbol{F}^{r2}$ path exhibits a more interesting behavior. Non-convexity of the rank-one convex hull is observed with a reduced non-convexity compared to $W(\boldsymbol{F})$ though. The presence of non-convexity allows the description of strain-softening when using the rank-one convex envelope, since the first derivative is decreasing after the point of inflection. Currently, the first derivative is computationally hard to obtain, since the algorithm relies on a linear interpolation that has no derivative at the interpolation points due to the presence of kinks. Furthermore, the second derivative, needed for a Newton–Raphson scheme, is not available.

In future investigations with respect to laminate depth, the acceleration of the algorithm by means of simplifications and parallelization as well as the reconstruction of derivatives will be examined.

4. Reconvexification

The multi-dimensional relaxation by means of rank-one convex hulls can describe strain softening due to the presence of non-convexity along paths with rank > 1. However, the construction is still rather expensive and the appropriate construction of derivatives is an open research question. Therefore, the relaxation is resorted to the one-dimensional case for now. The schemes of [10, 13] kept the convex hull fixed after loss of convexity because the evolution of the internal variable in the steps afterwards is simply unknown. In [19], the concept of *reconvexification* was introduced due to the possibility to construct the convex hull in each incremental step by the methods of [16]. Within the publication, the convex hull is constructed in each incremental step and the strongly damaged phase, associated with the deformation gradient F^+, is allowed to evolve. Interestingly, the evolution of the strongly damaged phase only changes the deformation gradient F^+ but the associated internal variable β^+ remains constant. This implies that the energetic level of the strongly damaged phase remains the same and, thus, it is in line with the concept of a mixture of two damaged phases. The two-element perturbation test has been carried out in [19] to show the distinct feature of strain softening, while providing mesh-independent solutions. This test is visualized at the right-hand side of Figure 2. The boundary value problem on the fixed interval $[0, L]$ consists of two elements where one material parameter is distorted by a small value ϵ. The individual lengths of the elements are characterized by the parameter κ. As can be seen from Figure 2, the response of the reconvexified model is mesh-independent while at the same time strain-softening is present. This is possible by solving subsequent convex problems with decreasing slope of the linear connection of the convex hull supporting points.

5. Conclusion and Outlook

In this contribution, two approaches were presented that enable the description of strain softening for relaxed incremental damage formulations. Within the multi-dimensional setting, numerical rank-one convexification was used that showed a remaining non-convexity along paths that have a higher rank than one. This non-convexity opens the possibility for the description of strain-softening even for a fixed convex hull. However, the construction of first and second derivatives is a challenging task that will be addressed in the future. Furthermore, simplifications can be tested with respect to the used rank-one direction discretization, since incremental stress potentials of continuum damage mechanics are smooth.

The multi-dimensional relaxation suffers from the curse of dimensionality and, thus, the one-dimensional reconvexified model of [19] has been presented as well. This model relies on one-dimensional convexification and enables the description of strain-softening by constructing the convex hull in each incremental step in combination with a decreasing

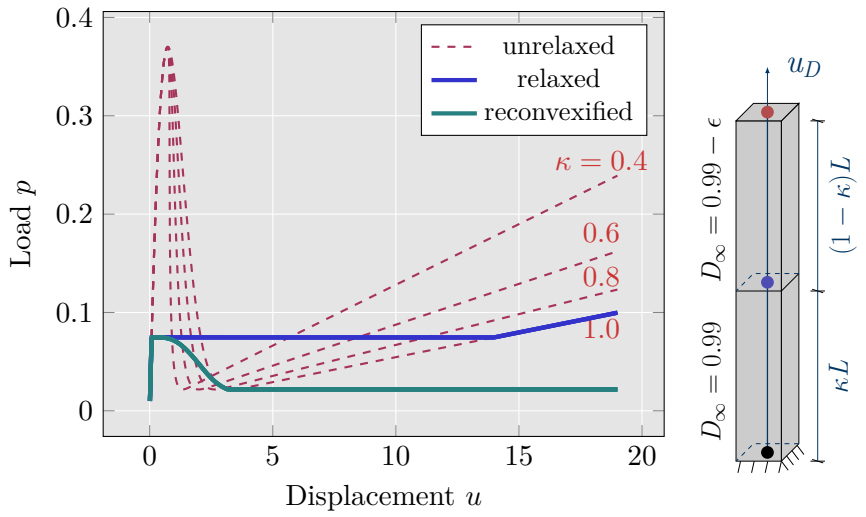

FIGURE 2. One-dimensional perturbation mesh independence test of mesh-dependent unrelaxed model, mesh-independent relaxed model of [13], and mesh-independent reconvexified model of [19].

slope of the convex hull. The mathematical analysis of this model remains an open research question and so does the extension of the approach to the multi-dimensional case. To sum up, relaxed incremental damage formulations are able to describe strain softening. For the description within relaxed damage models, two known options exists. In the higher dimensional case, weaker convexity notions appear to be sufficient for the description of strain softening; however, in the one-dimensional case the evolution of the microstructure is necessary.

REFERENCES

[1] K. Hackl, Journal of the Mechanics and Physics of Solids **45**(5), 667–688 (1997).

[2] M. Ortiz and L. Stainier, Computer Methods in Applied Mechanics and Engineering **171**(3), 419–444 (1999).

[3] M. Ortiz and E. Repetto, Journal of the Mechanics and Physics of Solids **47**(2), 397–462 (1999).

[4] C. Carstensen, K. Hackl, and A. Mielke, Proceedings of the Royal Society of London. Series A: Mathematical, Physical and Engineering Sciences **458**(2018), 299–317 (2002).

[5] A. Mielke, F. Theil, and V. I. Levitas, Archive for Rational Mechanics and Analysis **162**(2), 137–177 (2002).

[6] S. Bartels, Numerical Methods for Nonlinear Partial Differential Equations, Springer Series in Computational Mathematics, Vol. 47 (Springer International Publishing, Cham, 2015).

[7] T. Bartel and K. Hackl, ZAMM - Journal of Applied Mathematics and Mechanics / Zeitschrift für Angewandte Mathematik und Mechanik **89**(10), 792–809 (2009).

[8] S. Bartels, C. Carstensen, K. Hackl, and U. Hoppe, Computer Methods in Applied Mechanics and Engineering **193**(48-51), 5143–5175 (2004).

[9] M. Lambrecht, C. Miehe, and J. Dettmar, International Journal of Solids and Structures **40**(6), 1369–1391 (2003).

[10] E. Gürses and C. Miehe, Journal of the Mechanics and Physics of Solids **59**(6), 1268–1290 (2011).

[11] L. M. Kachanovp. 8 (1958).
[12] C. Miehe, European Journal of Mechanics A-solids(January) (1995).
[13] D. Balzani and M. Ortiz, International Journal for Numerical Methods in Engineering **92**(6), 551–570 (2012).
[14] T. Schmidt and D. Balzani, Journal of the Mechanical Behavior of Biomedical Materials **58**(May), 149–162 (2016).
[15] S. Schwarz, P. Junker, and K. Hackl, Continuum Mechanics and Thermodynamics(May) (2020).
[16] M. Köhler, T. Neumeier, J. Melchior, M. A. Peter, D. Peterseim, and D. Balzani, Acta Mechanica(September) (2022).
[17] G. Dolzmann and N. Walkington, Numerische Mathematik **85**(4), 647–663 (2000).
[18] S. Bartels, ESAIM: Mathematical Modelling and Numerical Analysis **38**(5), 811–820 (2004).
[19] M. Köhler and D. Balzani, arXiv(2208.14695) (2022), submitted.
[20] J. E. Marsden, T. J. R. Hughes, and D. E. Carlson, Journal of Applied Mechanics **51**(4), 946–946 (1984).
[21] R. V. Kohn and G. Strang, Communications on Pure and Applied Mathematics **39**(2), 139–182 (1986).